A New Restoration Algorithm for Single Image Defogging

Fan Guo, Hui Peng, and Jin Tang

School of Information Science and Engineering, Central South University, Changsha, China
guofancsu@163.com

Abstract. Fog is an atmospheric phenomenon that significantly degrades the visibility of outdoor scenes. Thus, this paper presents an algorithm to remove fog for a single image. The method estimates the transmission map of image degradation model by assigning labels with MRF model and optimizes the map estimation process using the graph-cut based α-expansion technique. The algorithm goes with two steps: first, the transmission map is estimated using a dedicated MRF model combined with the bilateral filter. Then, the restored image is obtained by taking the estimated transmission map and the airlight into the image degradation model to recover the scene radiance. A comparative study is proposed with a few other state of the art algorithms which demonstrate that better quality results can be obtained using the proposed method.

Keywords: image, restoration, fog removal, image degradation model, transmission map.

1 Introduction

The quality of photograph in our daily life is easily undermined by the aerosols suspended in the medium, such as dust, mist, or fumes. This has an effect on the image, e.g., contrasts are reduced and the surface color becomes fait. Such degraded photographs often lack visual vividness and offer a poor visibility of the scene contents. The goal of defogging algorithms is to enhance and recover the detail of the scene from foggy image. There are many circumstances that accurate fog removal algorithms are needed. In computer vision, most automatic systems for surveillance, intelligent vehicles, object recognition, etc., assume that the input images have clear visibility. However, this is not always true in bad weather. Therefore, removing fog from a single image is very important and useful. Since the process of image defogging depends on the depth of the scene, thus the essential problem that must be solved in most image defogging methods is scene depth estimation. This is not trivial and requires prior knowledge. In this paper, the transmission map is estimated by assigning labels with MRF model and optimizes the map estimation process using the graph-cut based α-expansion technique. Experimental results show that good defogging effect may be produced by using the proposed method.

Since the importance of the defogging algorithm, many defogging works have been done. Graphical model (GM), as a probabilistic model combined probability with graph, is an important way to solve this problem. The models can be divided into two

S. Li et al. (Eds.): CCPR 2014, Part II, CCIS 484, pp. 169–178, 2014.

types: directed graph and undirected graph. Generally, a directed GM is a Bayesian network (BN) when the graph is acyclic, meaning there are no loops in the directed graph. The relationships in a BN can be described by local conditional probabilities [1]. In [2, 3], a Bayesian defogging method that jointly estimates the scene albedo and depth from a single foggy image is introduced by leveraging their latent statistic structure. The undirected graph refers to Markov Random Field (MRF). Since MRF is undirected and may be cyclic, it can represent certain dependencies that a BN cannot, which providing a new way for image defogging due to the dependencies exist between the neighboring pixels. The defogging algorithm in [4] based on the observation that the surface Lambertian shading factor and the scene transmission are locally independent in order to separate the fog from the scene, and then a Gaussian-Markov random field is used to smooth the transmission values. In [5], a cost function in the framework of MRF is developed to enhance the visibility of the images. However, the results obtained by this method tend to have larger saturation values than those in the actual clear-day images. In [6], the scene geometry and the alpha-expansion optimization technique are employed to improve the robustness of single image dehazing algorithm. Recently, image defogging based on MRF model has made significant progresses [7-8]. In [7], the image defogging problem is decomposed into two steps: first infer the atmospheric veil using a dedicated MRF model, and second estimate the restored image by minimizing MRF energy. In this MRF model, the flat road assumption is introduced to achieve better results on road images. In [8], a MRF model of both stereo reconstruction and defogging problems is combined into a unified MRF model to take advantages of both stereo and atmospheric veil depth cues. Thus, the stereo reconstruction and image defogging in daytime fog can be solved using the new MRF model. In [9], a multi-level depth estimation method based on MRF model is presented for image defogging. The method integrated the characteristic of dark channel prior into the MRF model to estimate an accurate depth map. MRF is applied here to label the depth level in adjacent region for the compensation of wrong estimated regions. The textures in the scene are the critical element served as the smooth term in the MRF model. These fog removal algorithms are the most representative of MRF defogging methods. However, the color or the profile of the scene objects may sometimes look unnatural for the defogged results.

2 Background

2.1 Markov Random Field

Many vision problems can be naturally solved by using MRF technique. Markov random field theory is a branch of probability theory for analyzing the spatial or contextual dependencies of physical phenomena. It is often used in visual labeling to establish probabilistic distribution of interacting labels. Here, we use MRF to estimate the transmission map in image degradation model. It is an undirected graph, and adjacent nodes are connected to determine the depth of real scene [9]. We associate hidden layer with the dense level of fog and observation layer with the initial

transmission map, and then a MRF model is provided to a cost function as shown in follows:

$$E(f) = \sum_{p \in P} D_p(f_p) + \sum_{(p,q) \in N} V_{p,q}(f_p, f_q) \quad , \tag{1}$$

In (1), $f = \{f_p \mid p \in P\}$ is a labeling of image P, f_p is the label of pixel p in the image P, and f_p={1, 2, 3,…,k}. q is the neighbor of p, N is the set of pairs of pixels defined over the standard four-connection neighborhood. $E(f)$ is for minimizing sums of two types of terms. The first term $D_p(.)$ is a data function. The smaller difference between the pixel and its label, the smaller $D_p(.)$ will be. $D_p(.)$ penalizes a label f_p to pixel p if it is too different with the observed data I_p. Generally, the data term in MRF model or other energy function of regularization based optimization problem constructs the constraint between the expected variable and some known observations about the variable. The second term $V_{p,q}(.)$ is a smooth function (or called discontinuity-preserving) [10, 11]. The smaller difference among the labels of pixels in set N, the smaller $V_{p,q}(.)$ will be. $V_{p,q}(.)$ encourage the integrity of an image by penalizing two neighboring labels f_p and f_q if they are too different. The choice of $V_{p,q}(.)$ is a critical issue, and in the proposed defogging method we apply the geometry prior to obtain this term. With the smoothing term, the saturated colors at each pixel can be computed with a reasonable smoothing. Thus, for the transmission map estimation, the data function represents the probability of pixel p having transmission association with label f_p. The smooth function encodes the probability where neighboring pixels should have similar depth. For the transmission map estimated by using MRF model, the small value of the label on behalf of the deeper depth in the scene, vice versa. The relabeling results would be the initial transmission map of the proposed method. However, there still exists some redundant details need to be removed.

2.2 Geometry Prior for Foggy Image

In this section, we'll present the geometry prior that used in the transmission map estimation of the proposed algorithm. Light passing through a scattering medium is attenuated and distributed to other directions. This can happen anywhere along the path, and leads to a combination of radiances incident towards the camera. Formally, to express the relative portion of light that managed to survive the entire path between the observer and a surface point in the scene, the defined transmission map t_i combines the geometric distance d_i and medium extinction coefficient β (the net loss from scattering and absorption) into a single variable [12]: $t_i = e^{-\beta d_i}$. Thus, the following geometry prior is reasonable: assuming that β is constant over the image, the variations of transmission are due to the distance d between the scene point and the camera, and the larger distance means the smaller intensity in the transmission map. For most outdoor images, especially the surveillance images, the transmission map can be expressed in the component of distance along the ground and height above the ground. As long as the scene does not contain any cave-like surfaces, such as the space underneath a bridge, the distance along the ground to the visible scene point is a monotonically increasing function of image plane height which starts from

the bottom of image to the top. Therefore, the object which appears closer to the top of the image is usually further away. To verify the effectiveness of the geometry prior, we collect an outdoor image sets from internet and real captured photos. Statistical results show that about 83% images support our geometry prior. Since the geometry prior is a kind of statistic, it may not work for some particular images when the scene objects which near observer appear on the top of images, e.g., twigs, walls, trees, etc. the geometry prior is invalid. Fortunately, the proposed MRF-based method can still produce a reasonable transmission map without creating significant errors in the restored image.

3 The Proposed Algorithm

Specifically, the proposed algorithm has three steps to remove fog from a single image: the first one is computing the airlight according to the three distinctive features of sky region. The second step is computing the transmission map with the MRF model and the bilateral filter. The goal of this step is assigning the accurate pixel label using the graph-cut based α-expansion and removing the redundant details using the bilateral filter. Finally, with the estimated airlight and transmission map, the scene radiance can be recovered according to the image degradation model.

3.1 Airlight and Transmission Map Estimation

The presence of aerosols in the lower atmosphere means that the light may scatter and be absorbed while traveling through the medium [13]. This can happen anywhere along the path, and lead to a combination of radiances incident towards the camera. The image degradation model that widely used to describe the formation of the foggy image is as follows [2]:

$$I(\mathbf{x}) = J(\mathbf{x})t(\mathbf{x}) + A(1 - t(\mathbf{x})) \tag{2}$$

where $I(\mathbf{x})$ is the observed intensity corresponding to the pixel $\mathbf{x}=(x, y)$ and also the input foggy image, $J(\mathbf{x})$ is the scene radiance and also the fog removal image, A is the airlight, and $t(\mathbf{x})$ is the transmission map, which is the key factor for image defogging. In (2), the first term $J(\mathbf{x})t(\mathbf{x})$ is called direct attenuation model, and the second term $A(1- t(\mathbf{x}))$ is called airlight model. Theoretically, the goal of fog removal is to recover $J(\mathbf{x})$ from the estimated A, $t(\mathbf{x})$ and the original image $I(\mathbf{x})$.

3.1.1 Airlight Estimation

To estimate the airlight, we sum up the three distinctive features of sky region according to the nature fact of a large quantity of image sky regions. The distinctive features of sky region are: (i) bright minimal dark channel, (ii) flat intensity, and (iii) upper position. For the first feature, the pixels that belong to the sky region should satisfy $I_{min}(\mathbf{x}) > T_v$, where $I_{min}(\mathbf{x})$ is the dark channel and T_v is the 95% of the maximum value of $I_{min}(\mathbf{x})$. For the second feature, the pixels should satisfy the constraint $N_{edge}(\mathbf{x}) < T_p$

where $N_{edge}(\mathbf{x})$ is the edge ratio map and T_p is the flatness threshold. Due to the third feature, the sky region can be determined by searching for the first connected component from top to bottom. Thus, the atmospheric light A is estimated as the maximum value of the corresponding region in the foggy image $I(\mathbf{x})$. Fig. 1 shows the contrastive airlight estimation result for comparing the performance of the proposed sky region detection with the "brightest pixel" method. From Fig. 1, we can see that the proposed technique is more robust than the "brightest pixel" method. Notice that the proposed technique can gracefully handle the input foggy images even without sky regions by using the image degradation and MRF model. If not so, other methods, such as contrast enhancement, can be used to remove fog from input images.

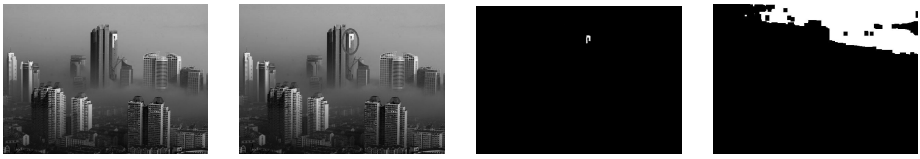

(a) (b) (c) (d)

Fig. 1. Airlight estimation example. (a) Input image. (b) The brightest pixels region. (c) The wrong sky region obtained by the "brightest pixel" method. (d) The correct sky region obtained by the proposed method.

3.1.2 Initial Transmission Map Estimation

Transmission map estimation is the most important step for image defogging, here we use the graph-cut based α-expansion method to estimate the map $t(\mathbf{x})$, as it is able to handle regularization and optimization problem, and has a good track record with vision-specific energy function [14]. Specifically, each elements t_i of the transmission map is associated with a label x_i, where the set of Labels $L=\{0, 1, 2, \ldots, l\}$ represents the transmission values $\{0, 1/l, 2/l, \ldots, 1\}$. Before labeling, we first convert input RGB image to gray-level image. Thus, the number of Labels is 32 since the labeling unit of pixel value is set to be 8 and l=31. The most probable labeling x^* minimizes the associated energy function:

$$E(x) = \sum_{i \in P} E_i(x_i) + \sum_{(i,j) \in N} E_{ij}(x_i, x_j) \tag{3}$$

where P is the set of pixels in the unknown transmission t, and N is the set of pairs of pixels defined over the standard four-connect neighborhood. The unary function $E_i(x_i)$ is the data term representing the possibility of pixel i having transmission t_i associated with label x_i. The smooth term $E_{ij}(x_i, x_j)$ encodes the possibility where neighboring pixels should have similar depth.

For data function $E_i(x_i)$, which represents the possibility of pixel i having transmission t_i associated with label x_i, we first convert the input RGB image I_i to gray-level image $I_i^{'}$, and then compute the absolute differences between each pixel value and the label value. The process can be written as:

$$E_i(x_i) = \left| I_i^{'} \times \omega - L(x_i) \right| \tag{4}$$

In (4), $I_i^{'}$ is the intensity of pixel in the gray-level image ($0 \le I_i^{'} \le 1$). $L(x_i)$ is the each element in the set of Labels $L=\{0, 1/l, 2/l, \ldots, 1\}$. The parameter ω is introduced to ensure that $I_i^{'}$ and $L(x_i)$ have same order of magnitude. Since each pixel value of our initial transmission map is expressed by the label x_i, and the labels depend on the pixel intensity of gray-level image. Thus, the data function can model two different physical quantities together, i.e., pixel intensity and transmission.

The smooth function $E_{ij}(x_i, x_j)$ encodes the possibility where neighboring pixels should have similar depth. Inspired by the work [6], we use the linear cost function, which is solved by α-expansion:

$$E_{ij}(x_i, x_j) = w \left| x_i - x_j \right| \tag{5}$$

From the geometry prior, we know that objects which appear closer to the top of the image are usually further away. Thus, if we consider two pixels i and j, where j is directly above i, we have $d_j > d_i$ according to the geometry prior. Thus, we can deduce that the transmission t_j of pixel j must be less than or equal to the transmission t_i of pixel i, that is $x_j \le x_i$. For any pair of labels which violate this trend, a cost $c>0$ can be assign to punish this pattern. Thus, the smooth function in Eq. (5) can be written as:

$$E_{ij}(x_i, x_j) = \begin{cases} c & if \ \ x_i < x_j, \\ w \left| x_i - x_j \right| & otherwise. \end{cases} \tag{6}$$

The parameters w and c are used to control the aspect of defogging effect. The value of w controls the strength of the detail enhancement, and is usually set to 0.01. The cost c controls the strength of the color recovery, and is usually set to 100. The two parameters are useful to compromise between highly enhanced details where colors may appear too dark, and less restored details where colors are brighter. Besides, the weights associated with the graph edge should be determined. If the intensity of two neighboring pixels in the input foggy image I are less than 15 in each channel, which means the two pixels have high possibility of sharing the same transmission value. Thus, the cost of the labeling is increased by 15× to minimize the artifacts due to the depth discontinuities in this case. Taking the data function and the smooth function into the energy function equation (3), the pixel label of transmission map can be estimated by using the graph-cut based α-expansion. In our method, the gco-v3.0 library [14] developed by Veksler *et al*. is adopted for optimizing multi-label energies via the α-expansion. It supports energies with any combination of unary, pairwise, and label cost terms [15, 16]. Thus, we use the library to estimate each pixel label in initial transmission map. By using the functions defined in the optimization library, we can obtain each pixel label x_i. Then, a proper intensity value of the initial transmission map can be assigned to each image pixel. Specifically, for each label x_i, we have

$$t_{ini}(\mathbf{x}) = 255 - (x_i - 1) \times 8 \tag{7}$$

In Eq. (7), t_{ini} is the initial transmission map estimated by the proposed MRF-based algorithm. An illustrative example is shown in Fig. 2. In the figure, Fig. 2(b) shows the initial transmission map estimated using the algorithm presented above, its corresponding restored result is shown in Fig. 2(c). One can clearly see that the appearance of the scene objects in the restored image looks one-dimensional.

(a) (b) (c) (d) (e)

Fig. 2. True example. (a) Input image. (b) Initial transmission map. (c) Restored result obtained using (b). (d) Bilateral filter to (b). (e) Restored result obtained using (d).

3.1.3 Refined Transmission Map Estimation

As shown in Fig. 2, there is obvious deficiency in the recovered image in the discontinuities of the transmission map obtained by MRF model. For example, the red bricks and the slots between them should have the same depth values. However, as shown in Fig. 2(b), one can clearly see the slots between the bricks in transmission map estimated by the MRF-based algorithm. In order to handle these discontinuities, many works adopt the bilateral filter to refine the transmission map estimation. Thus, the redundant details of the transmission map t_{ini} estimated by the algorithm presented above can be effectively removed, which improves the restored result with better detail enhancement capability. This process can be written as:

$$t(\boldsymbol{u}) = \frac{\sum_{\boldsymbol{p}\in N(\boldsymbol{u})} W_c(\|\boldsymbol{p}-\boldsymbol{u}\|) W_s(|t_{ini}(\boldsymbol{u}) - t_{ini}(\boldsymbol{p})|) t_{ini}(\boldsymbol{p})}{\sum_{\boldsymbol{p}\in N(\boldsymbol{u})} W_c(\|\boldsymbol{p}-\boldsymbol{u}\|) W_s(|t_{ini}(\boldsymbol{u}) - t_{ini}(\boldsymbol{p})|)} \tag{8}$$

where $t_{ini}(\boldsymbol{u})$ is the initial transmission map corresponding to the pixel $\boldsymbol{u}=(x, y)$, $N(\boldsymbol{u})$ is the neighbors of $\mathbf{u}$. The spatial domain similarity function $W_c(x)$ is a Gaussian filter with the standard deviation σ_c : $W_c(x) = \mathrm{e}^{-x^2/2\sigma_c^2}$, and the intensity similarity function $W_s(x)$ is a Gaussian filter with the standard deviation σ_s, it can be defined as: $W_s(x) = \mathrm{e}^{-x^2/2\sigma_s^2}$. In our experiments, the value of σ_c and σ_s is set as 3 and 0.4, respectively. Thus, we can obtain the final refined transmission map, as shown in Fig. 2(d), and Fig. 2(e) is the restored result obtained using the refined map. From Fig. 2(e), one can see that the restored result obtained using the bilateral filter has more layer and stereoscopic feelings compared with the result [see Fig. 2(c)] obtained without using the filter.

3.2 Scene Radiance Recovery

Since now we already know the input haze image $I(\mathbf{x})$, the final refined transmission map $t(\mathbf{x})$ and the airlight A, we can obtain the final fog removal image $J(\mathbf{x})$ according to the image degradation model. The final defogging result $J(\mathbf{x})$ is recovered by:

$$J(\mathbf{x}) = \frac{I(\mathbf{x}) - A}{\max(t(\mathbf{x}), t_0)} + A \tag{9}$$

where t_0 is application-based, and it is used to adjust the fog kept at only the farthest reaches of the image. If the value of t_0 is too large, the result has little defogging effect, and if the value is too small, the color of fog removal result seems oversaturated. Experiment shows that when t_0 is set to be 0.2, we can get visual pleasing results in most cases.

4 Experimental Results

To evaluate the performance of various defogging algorithms, we compared our defogging algorithm with a few other state of the art algorithms. The first image of Fig. 3(b) shows the defogging result obtained by Fattal [17]. As can be seen in the figure, Fattal's method can produce a visual pleasing result. However, the method is based on statistics and requires sufficient color information and variance. If the fog is dense, the color information used in that method is not enough to reliably estimate the transmission. Then, we compare our method with Tan's work [18] in the second images of Figs. 3(b) and 3(d). The colors of Tan's result may sometimes over saturate or distort. For example, the color of the sky and road region in the Tan's result is turned into yellow, as shown in the figure. We also give He's work [19] in the third images of Fig. 3(b). He's algorithm can achieve a good enhancement effect for most outdoor images. However, when the scene objects are inherently similar with the airlight, the dark channel prior used in He's method will be invalid. In this case, the defogging result of He's algorithm is not visual pleasing, as shown in Fig. 3(b). The fourth images of Figs. 3(b) and 3(d) show a comparison between results obtained by Carr [6] and our algorithm. It can be seen that our algorithm tend to enhance details better than Carr's result, and the color of our result seems more close to the original input image. The fifth and sixth images of Figs. 3(b) and 3(d) show the results of our method and Caraffa's methods [7, 8]. From these images, we can see that although the results we get can't thoroughly remove the fog in very dense fog regions compared with Caraffa's methods, such as the buildings and the trees far away, our results appear natural in both color and the profile of the scene objects. The seventh images of Figs. 3(b) and 3(d) show a comparison between results obtained by Wang [9] and our method. One can clearly see that the color of the sky region in Wang's result seems a little inconsistent with that of the original foggy image. Experiments on a large quantity of outdoor images confirm the above conclusions. Since transmission map is very important to recover a good result, we also present the estimated transmission maps in Fig. 3(c).

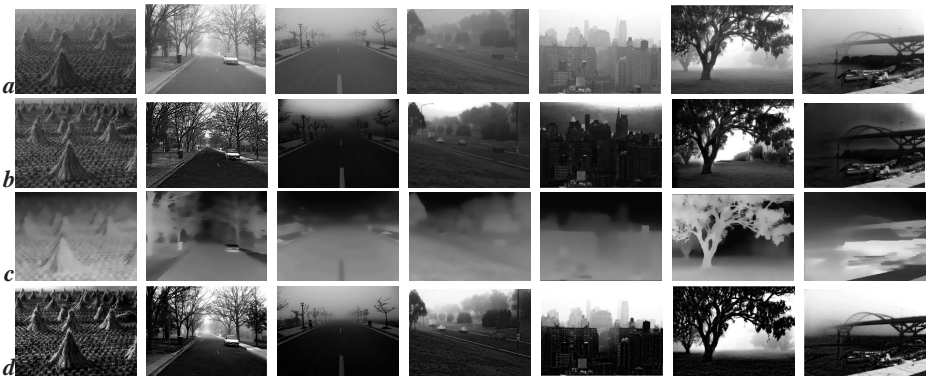

Fig. 3. The comparison between recent fog removal work. (a) Original foggy images. (b) Corresponding fog removal results obtained by recent defogging algorithms. From left to right: Fattal's, Tan's, He's, Carr's, Caraffa's and Wang's results. (c) Our estimated transmission map. (d) Our fog removal results.

Therefore, results on a variety of haze or fog images show that the defogging image obtained with our algorithm seems visually close to the result obtained by Fattal, He and Carr, with better color fidelity and less halo artifacts compared with Tan, Caraffa and Wang. For our proposed algorithm, it takes about 2 minute to process a 600×400 pixel image. Notice that when the image size is small, the proposed method has a relatively faster speed. For example, only 3 second is needed to process a 250×190 pixel image using the proposed method. All the algorithms are tested by executing MATLAB on a PC with 3.00GHz Intel Pentium Dual-Core Processor. The speed can be further improved by using efficient parallel computation with a GPU.

5 Conclusion

Image defogging is an important issue in computer vision. In this paper, a new defogging algorithm was presented based on MRF model. The problem was formulated as estimation of transmission map with α-expansion optimization. The algorithm is implemented by two steps: the transmission map is first estimated using a dedicated MRF model and the bilateral filter. Once the map is inferred, the restored image can be obtained according to the image degradation model. Experimental results demonstrate that the proposed algorithm can produce visually pleasing defogging results and tend to enhance the image contrast, which is better than previous techniques. However, the color of our defogging results sometimes seemed over-saturated. Nevertheless, we could improve the overall quality of a foggy image by enhancing the main details, and the algorithm could be further improved by employing better prior for the data and smooth function of the MRF model. In the future, we intend to investigate the case of various kinds of fog and speed up the proposed algorithm for real-time processing.

Acknowledgments. This work was supported by the National Natural Science Foundation of China (71271215, 71221061, and 91220301), the International Science & Technology Cooperation Program of China (2011DFA10440), and the Collaborative

Innovation Center of Resource-conserving & Environment-friendly Society and Ecological Civilization, the China Postdoctoral Science Foundation (No. 2014M552154), the Hunan Postdoctoral Scientific Program (No. 2014RS4026), and the Postdoctoral Science Foundation of Central South University (No. 126648).

References

1. Li, S.Z.: Markov random field modeling in image analysis, p. 21. Springer-Verlag London Limited, UK (2009)
2. Nishino, K., Kratz, L., Lmbardi, S.: Bayesian defogging. International Journal of Computer Vision 98(3), 263–278 (2012)
3. Kratz, L., Nishino, K.: Factorizing scene albedo and depth from a single foggy image. In: IEEE International Conference on Computer Vision (ICCV), pp. 1701–1708 (2009)
4. Fattal, R.: Single image dehazing. ACM Transactions on Graphics 27(3), 1–9 (2008)
5. Tan, R.T.: Visibility in bad weather from a single image. In: IEEE International Conference on Computer Vision and Pattern Recognition (CVPR), pp. 1–8 (2008)
6. Carr, P., Hartley, R.: Improved single image dehazing using geometry. In: The Digital Image Computing: Technique and Applications, Melbourne, pp. 103–110 (2009)
7. Cataffa, L., Tarel, J.P.: Markov random field model for single image defogging. In: IEEE Intelligent Vehicle Symposium, pp. 994–999 (2013)
8. Caraffa, L., Tarel, J.-P.: Stereo reconstruction and contrast restoration in daytime fog. In: Lee, K.M., Matsushita, Y., Rehg, J.M., Hu, Z. (eds.) ACCV 2012, Part IV. LNCS, vol. 7727, pp. 13–25. Springer, Heidelberg (2013)
9. Wang, Y.K., Fan, C.T., Chang, C.W.: Accurate depth estimation for image defogging using Markov Random Field. In: International Conference on Graphic and Image Processing (ICGIP), Singapore, pp. 1–5 (2012)
10. Kolmogorov, V., Zabin, R.: What energy function can be minimized via graph cuts? IEEE Transactions on Pattern Analysis and Machine Intelligence (PAMI) 26(2), 147–159 (2004)
11. Boykoc, Y., Kolmogorov, V.: An experimental comparison of Min-cut/Max-flow algorithms for energy minimization in vision. IEEE Transactions on Pattern Analysis and Machine Intelligence (PAMI) 26(9), 1124–1137 (2004)
12. Rossum, M.V., Nieuwenhuizen, T.: Multiple scattering of classical waves: microscopy, mesoscopy and diffusion. Reviews of Modern Physics 71(1), 313–371 (1999)
13. Narasimhan, S.G., Nayar, S.K.: Vision and the atmosphere. International Journal on Computer Vision 48(3), 233–254 (2002)
14. The gco-v3.0 library (gco-v3.0), `http://vision.csd.uwo.ca/code/` (accessed April 5, 2013)
15. Boykov, Y., Veksler, O., Zabin, R.: Fast approximate energy minimization via graph cuts. IEEE Transaction on Pattern Analysis and Machine Intelligence (PAMI) 23(11), 1222–1239 (2001)
16. Delong, A., Osokin, A., Isack, H.N., Boykov, Y.: Fast Approximate Energy Minimization with Label Costs. International Journal of Computer Vision 96(1), 1–27 (2012)
17. Fattal, R.: Single image dehazing, ACM Transactions on Graphics (SIGGRAPH 2008) 27, 72:1–72:9 (2008)
18. Tan, R.T.: Visibility in bad weather from a single image. In: IEEE Conference on Computer Vision and Pattern Recognition (CVPR), United States, pp. 1–8 (2008)
19. He, K.M., Sun, J., Tang, X.O.: Single image haze removal using dark channel prior. IEEE Transactions on Pattern Analysis and Machine Intelligence 33(12), 2341–2353 (2011)